Conserved role for Gga proteins in phosphatidylinositol 4-kinase localization to the *trans*-Golgi network

Lydia Daboussi[a,1], Giancarlo Costaguta[a,1], Razmik Ghukasyan[a], and Gregory S. Payne[a,2]

[a]Department of Biological Chemistry, David Geffen School of Medicine, University of California, Los Angeles, CA, 90095

Edited by Jeremy W. Thorner, University of California, Berkeley, CA, and approved February 13, 2017 (received for review September 9, 2016)

Phosphoinositides serve as key membrane determinants for assembly of clathrin coat proteins that drive formation of clathrin-coated vesicles. At the *trans*-Golgi network (TGN), phosphatidylinositol 4-phosphate (PtdIns4P) plays important roles in recruitment of two major clathrin adaptors, Gga (Golgi-localized, gamma-adaptin ear homology, Arf-binding) proteins and the AP-1 (assembly protein-1) complex. The molecular mechanisms that mediate localization of phosphatidylinositol kinases responsible for synthesis of PtdIns4P at the TGN are not well characterized. We identify two motifs in the yeast phosphatidylinositol 4-kinase, Pik1, which are required for binding to the VHS domain of Gga2. Mutations in these motifs that inhibit Gga2–VHS binding resulted in reduced Pik1 localization and delayed accumulation of PtdIns4P and recruitment of AP-1 to the TGN. The Pik1 homolog in mammals, PI4KIIIβ, interacted preferentially with the VHS domain of GGA2 compared with VHS domains of GGA1 and GGA3. Depletion of GGA2, but not GGA1 or GGA3, specifically affected PI4KIIIβ localization. These results reveal a conserved role for Gga proteins in regulating phosphatidylinositol 4-kinase function at the TGN.

clathrin | Gga adaptors | phosphatidylinositol 4-kinase | phosphatidylinositol 4-phosphate | *trans*-Golgi network

Clathrin-coated vesicles (ccv) are fundamental elements of protein transport pathways from the plasma membrane and between the *trans*-Golgi network (TGN) and endosomes in eukaryotic cells. Clathrin adaptors serve as central hubs in the physical and functional networks that drive ccv biogenesis. In particular, adaptors anchor the clathrin coat scaffold to the membrane, collect cargo, and recruit accessory factors that contribute to multiple steps in vesicle formation, including membrane invagination and vesicle release (1–3).

According to current paradigms, clathrin adaptors are recruited to the appropriate membrane through coincident low-affinity interactions with different targets (3, 4). In this process, phosphoinositides function as key membrane-specific determinants. At the TGN, phosphatidylinositol 4-phosphate (PtdIns4P) provides this function. The primary TGN adaptors—the heterotetrameric AP-1 (assembly protein-1) complex, GGA (Golgi-localized, gamma-adaptin ear homology, Arf-binding) proteins, and epsin-related proteins (epsinR in mammals, Ent3 and Ent5 in yeast)—preferentially bind PtdIns4P and/or are dependent on PtdIns4P for optimal localization and dynamics (5–10).

Although PtdIns4P-binding is recognized as important for clathrin adaptor function, relatively little is known about mechanisms that couple PtdIns4P synthesis to ccv formation. We have described a role for PtdIns4P in controlling sequential assembly of adaptor-specific ccv at the TGN in yeast (5), which correlates with sequential cargo-sorting events (11). The assembly sequence, termed adaptor progression, initiates with a wave of ccv enriched for Gga proteins and Ent3. A second ccv wave follows roughly 10 s later, enriched for AP-1 and Ent5. PtdIns4P regulates adaptor progression; reduced PtdIns4P levels disrupted progression, whereas increased rates of PtdIns4P accumulation shortened the time between adaptor waves. Identification of an interaction between the predominant yeast GGA protein, Gga2p, and the phosphatidylinositol 4-kinase (PI4K) responsible for TGN PtdIns4P production, Pik1, suggested a possible mechanism for coupling PtdIns4P synthesis to clathrin coat assembly. Consistent with this model, deletion of yeast *GGA* genes delayed Pik1 recruitment to the TGN, accumulation of PtdIns4P, and assembly of AP-1. Here we define two Gga-binding motifs in Pik1 that are important for Pik1 recruitment and adaptor progression. Additionally, we present evidence that GGA proteins mediate recruitment of PI4KIIIβ to TGN in mammalian cells. Our results support a conserved function for GGA proteins in localizing PI4K to the TGN.

Results

Pik1 Sequences that Mediate Direct Binding to the Gga2–VHS Domain. In prior work (5), the interaction between Gga2 and Pik1 was mapped to the Gga2–VHS domain, which binds to a region of Pik1 that spans amino acids 80–760. To more precisely define VHS binding sites in this region of Pik1, we assessed direct binding of smaller Pik1 fragments to Gga2–VHS. Because of insolubility of fragments containing N-terminal sequences, we first focused on a region between amino acids 283 and 760 (Fig. 1*A*). Pik1 amino acids 283–425 clearly bound to Gga2–VHS, whereas Pik1 amino acids 410–760 binding was barely detectable, delineating the major interaction to amino acids 283–410. Amino-terminal truncation of Pik1 amino acids 283–425 to amino acid 301 abolished binding, indicating that sequences between amino acids 283 and 301 mediate interaction with Gga2–VHS. Sets of three adjacent amino acids spanning this region were mutated to alanines in Pik1 amino acids 283–425 and tested for binding to Gga2–VHS (Fig. 1*B*). Interaction was eliminated by triplet mutations across amino

Significance

Clathrin-coated vesicles (ccv) are fundamental intracellular transport carriers in eukaryotic cells. Assembly of ccv at appropriate intracellular membrane sites requires membrane-associated factors, including phosphoinositide lipids that recruit clathrin adaptors to the membrane to initiate ccv formation. How levels of specific phosphoinositides are controlled at particular membranes is not well understood. At the *trans*-Golgi network (TGN), the key phosphoinositide is phosphatidylinositol 4-phosphate (PtdIns4P). Here we characterize molecular interactions between Gga (Golgi-localized, gamma-adaptin ear homology, Arf-binding) clathrin adaptors and a kinase responsible for PtdIns4P synthesis at the TGN in yeast and mammalian cells. Defects that reduce kinase binding to Gga proteins inhibit kinase recruitment to the TGN. These results identify an evolutionarily conserved role for Gga clathrin adaptors in controlling PtdIns4P synthesis at the TGN.

Author contributions: L.D. and G.S.P. designed research; L.D., G.C., and R.G. performed research; L.D. and G.C. contributed new reagents/analytic tools; L.D., G.C., R.G., and G.S.P. analyzed data; and L.D., G.C., and G.S.P. wrote the paper.

The authors declare no conflict of interest.

This article is a PNAS Direct Submission.

[1]Present address: Gene Expression Laboratory, Salk Institute for Biological Studies, La Jolla, CA 92037.

[2]To whom correspondence should be addressed. Email: gpayne@mednet.ucla.edu.

This article contains supporting information online at www.pnas.org/lookup/suppl/doi:10.1073/pnas.1615163114/-/DCSupplemental.

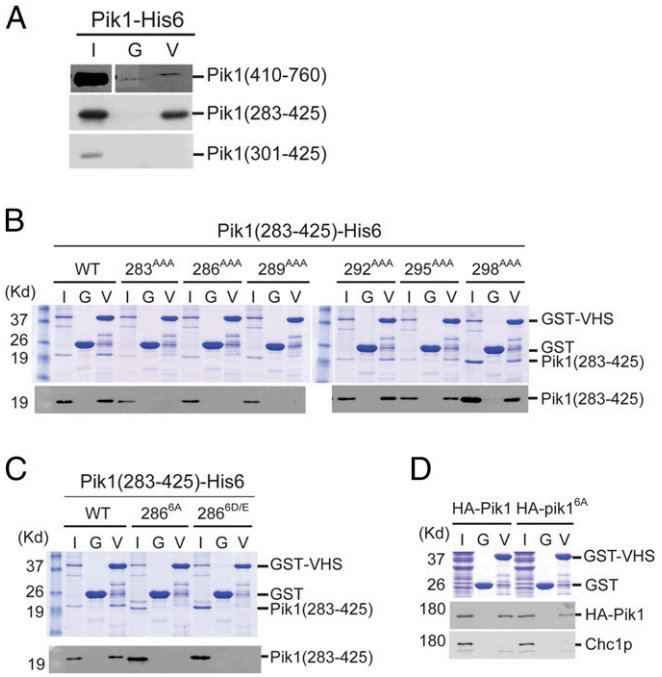

Fig. 1. Identification of a Gga2–VHS binding site in Pik1. (*A*) Pik1(283–425) directly binds Gga2–VHS. Purified fragments of Pik1-His6 were incubated with GST (G) or GST-Gga2–VHS (V) immobilized on glutathione-Sepharose. Bound proteins were eluted and analyzed by SDS/PAGE and immunoblotting with His tag antibody. Input (I) represents 8% of the sample used for binding. (*B*) Residues in Pik1(283–425) required for Gga2–VHS binding. Pik1 (283–425) mutants were tested for binding to Gga2–VHS as described in *A*. Bound proteins were detected by staining with Coomassie blue (*Upper*) or immunoblotting with His tag antibody (*Lower*). Input (I) = 2%. (*C*) Mutation of residues 286–291 in Pik1(283–425) eliminates binding to Gga2–VHS. Pik1 (283–425) mutants were tested for binding to Gga2–VHS as described in *B*. (*D*) Residues 286–291 are not required for binding of full-length Pik1 to Gga2–VHS. Lysates from strains overexpressing HA-tagged WT Pik1 (HA-Pik1, GPY4966) or Pik1 containing $(286–291)^{6A}$ mutations (HA-pik1^{6A}, GPY5063) were incubated with GST (G) or GST–VHS (V) on glutathione-Sepharase and bound proteins were analyzed by SDS/PAGE and staining with Coomassie blue (*Top*), immunoblotting with antibody to the HA tag (*Middle*) or clathrin heavy chain (Chc1p; *Bottom*). Input (I) = 2%.

acids 283–291, but not amino acids 292–300. The sequence of amino acids 283–291, which we term VHS binding site 2 (VBS2), is characterized by basic amino acids and prolines (Fig. S1). Alanine substitution of individual amino acids in VBS2 had little effect on VHS binding (Fig. S2*A*), suggesting that the remaining contacts between VBS2 and VHS in each mutant are sufficient for interaction. Consequently, we generated two mutants containing either acidic amino acids (6D/E) or alanines (6A) in place of VBS2 amino acids 286–291 (Fig. S1*B*). When present in Pik1 amino acids 283–425, these mutations completely disrupted binding to Gga2–VHS (Fig. 1*C*).

To determine whether VBS2 is necessary for VHS binding by full-length Pik1, the 6A or 6D/E VBS2 mutations were introduced into the chromosomal *PIK1* locus in yeast, modified to overexpress HA-tagged protein to facilitate binding analysis. The mutations had minimal effects on binding to Gga2–VHS (Fig. 1*D* and Fig. S2*B*), suggesting additional Gga2–VHS binding sites in Pik1.

A fragment of Pik1, amino acids 200–350, which carried the VBS2-inactivating 6D/E mutations, bound Gga2–VHS, providing evidence for another VHS binding site between amino acids 200 and 283 (Fig. 2*A*). Amino-terminal truncation of the amino acids 200–350 fragment through amino acid 214 did not affect Gga2–VHS binding, but interaction was eliminated by a truncation extending through amino acid 229, locating the binding site between amino acids 215 and 229 (Fig. 2*A*). Following the strategy used to define VBS2, triplet alanine substitutions in Pik1 fragment amino acids $215–325^{6D/E}$ identified amino acids 218–226 as critical for Gga2–VHS binding (Fig. 2*B*). This sequence, termed VBS1, is similar to VBS2 in the enrichment of basic amino acids (Fig. S1*B*). Conversion of all of the VBS1 basic amino acids to alanine (KR→A) abolished Gga2–VHS binding (Fig. 2*B*). In contrast to VBS2, substitution of single basic amino acids with alanine caused substantial defects in VBS1 binding to Gga2–VHS (Fig. S2*C*). Thus, VBS1 is more dependent on individual basic residues than VBS2.

Consistent with redundant binding sites, mutational inactivation of both VBS1 (218–220 KKT to EEA) and VBS2 (6D/E), but neither alone, prevented interaction of Pik1 amino acids 215–315 with Gga2–VHS (Fig. 2*C*). These mutations were then introduced into yeast cells overexpressing full-length HA-tagged Pik1 (HA-pik1^{gga}). We also generated a similar strain overexpressing a mutant (HA-pik1^{A-3A}) that harbors a less extensive array of alanine mutations in VBS1 (K218A) and VBS2 (PKR286-288AAA), modeled on mutations that strongly affected binding of the single sites to Gga2–VHS (Fig. 1*B* and Fig. S2*C*). Compared with WT, HA-pik1^{gga} binding to Gga2–VHS was reduced nearly 10-fold, whereas HA-pik1^{A-3A} binding decreased by 3-fold (Fig. 2*D*). Taken together, these data provide evidence that VBS1 and VBS2 serve as key sites for direct interaction of Pik1 with Gga VHS domains.

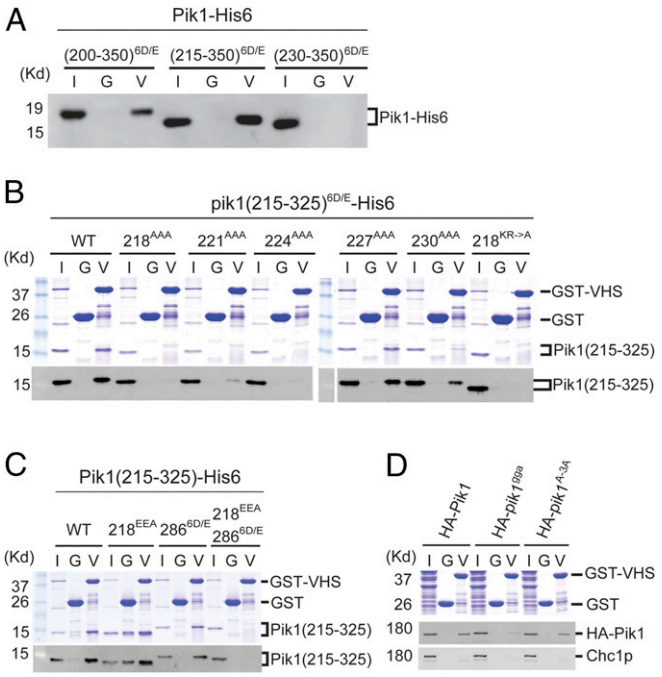

Fig. 2. VBS1 and VBS2 are major determinants of Pik1 binding to Gga2–VHS. (*A*) Identification of a second Gga2–VHS binding site in Pik1. Purified Pik1-His6 fragments, all bearing $(286–291)^{6D/E}$ mutations, were tested for binding to Gga2–VHS as in Fig. 1*A*. (*B*) Residues in Pik1$(215–325)^{6D/E}$ required for Gga2–VHS binding. Pik1$(215–325)^{6D/E}$ fragments carrying the indicated mutations were tested for binding to Gga2–VHS as in Fig. 1*B*; the KR→A mutant carries mutations of all positive residues in amino acids 218–225 to alanines. (*C*) The two Gga2–VHS binding sites in Pik1(215–325) are redundant. Pik1(215–325) mutants were tested for binding to Gga2–VHS as described in Fig. 1*B*. (*D*) Gga2–VHS binding to full-length Pik1 is reduced by mutation of both VBS1 and VBS2. Lysates from strains overexpressing HA-tagged WT Pik1 (HA-Pik1, GPY4966), HA-Pik1 containing $(218–220)^{EEA}$ and $(286–291)^{6D/E}$ mutations (HA-pik1^{gga}, GPY5062), or HA-Pik1 containing $(218)^{A}$ and $(286–288)^{3A}$ mutations (HA-pik1^{A-3A}, GPY5061) were tested for binding to Gga2–VHS as in Fig. 1*D*.

VBS1 and VBS2 Are Required for PtdIns4P Accumulation and Adaptor Recruitment. Levels of PtdIns4P play a critical role in controlling the temporal sequence of Gga and AP-1 recruitment to the TGN (5). We have proposed that Gga-mediated recruitment of Pik1 initiates this adaptor progression, based on observations that Pik1 binds to the Gga VHS domain, and that deletion of *GGA* genes delays Pik1 localization, PtdIns4P accumulation, and the subsequent recruitment of AP-1 at the TGN. To provide a more specific test of this hypothesis, we used live-cell imaging to characterize cells expressing the Gga-binding–defective VBS1/2 mutants of Pik1. For this purpose, the *pik1*^{gga} or *pik1*$^{A\text{-}3A}$ mutations were introduced into the *PIK1* locus and haploid strains generated so that the mutant alleles were expressed from the native promoter as the sole source of *PIK1*. In strains engineered to express Pik1 with an N-terminal epitope tag, mutant and WT proteins were present at similar levels (Fig. S3*A*).

Consistent with a role for Gga–VHS binding in Pik1 recruitment to the TGN, the intensity of fluorescent puncta in GFP–pik1$^{A\text{-}3A}$ cells was lower than in cells expressing GFP–Pik1 (Fig. 3 *A* and *B*). Unexpectedly, we were unable to generate cells expressing GFP–pik1^{gga}. Because neither GFP–Pik1 nor HA-tagged pik1^{gga} by themselves had significant effects on growth, this result suggests that the presence of a bulky GFP moiety at the N terminus has a synergistic impact on Pik1 function when combined with the charge reversal mutations in pik1^{gga}. Accordingly, in all subsequent experiments in yeast, we analyzed strains expressing untagged pik1$^{A\text{-}3A}$ and pik1^{gga}. Attempts to measure the dynamics of GFP–pik1$^{A\text{-}3A}$ mutants were hindered by a slight decrease in fluorescent intensity compared with WT GFP–Pik1, which is expressed at levels that yield puncta intensities near the threshold needed for temporal comparison with other TGN markers.

Accumulation of PtdIns4P was monitored in live cells expressing the TGN marker Sec7-mRFP and the PtdIns4P reporter GFP–PH^{OSH1}. In WT cells, Sec7-mRFP appears first in puncta, reaching peak intensity with an average time of 3.9 s ± 0.6 s (n = 41 puncta) before the peak in GFP–PH^{OSH1} fluorescence (Fig. 3*C* and Fig. S3*B*), in agreement with previous results (5). By comparison, a marked delay in GFP–PH^{OSH1} recruitment was evident in both *pik1* mutants, with average peak intensities reached 8.7 s ± 1.0 s (*pik1*^{gga}; $P = 7.8 \times 10^{-5}$, n = 51 puncta) and 11.3 s ± 1.9 s (*pik1*$^{A\text{-}3A}$; $P = 1.2 \times 10^{-3}$, n = 18 puncta), after the peak of Sec7-mRFP (Fig. 3*C* and Fig. S3*B*). Although there are differences in vitro between pik1^{gga} and pik1$^{A\text{-}3A}$ binding to the VHS domain of GGA, within the resolution of our analysis there was no statistical significance between pik1^{gga} and pik1$^{A\text{-}3A}$ effects on GFP-PH^{OSH1} dynamics (P = 0.23). We suspect that variation in peak-to-peak times within a strain may obscure in vivo differences between the two mutant strains caused by different levels of Gga2–VHS binding. Overall, the defects in GFP–PH^{OSH1} recruitment are concordant with delays reported for *gga1Δ gga2Δ* cells (11.3 s ± 0.9 s) (5), providing evidence that Pik1 binding to Gga proteins contributes to localized generation of PtdIns4P at the TGN.

In cells lacking Gga proteins, the slow accumulation of PtdIns4P is accompanied by a delay in AP-1 recruitment relative to Sec7 (5). Similarly, in *pik1* mutant cells expressing Sec7-mRFP and the AP-1 subunit β1-GFP, the average times between peaks of Sec7 and AP-1 were lengthened compared with WT cells: 11.6 s ± 1.4 s for WT (n = 27 puncta); 16.8 s ± 1.7 s for *pik1*^{gga} (P = 0.02, n = 47 puncta); 19.4 s ± 1.5 s for *pik1*$^{A\text{-}3A}$ ($P = 5.3 \times 10^{-4}$, n = 19 puncta) (Fig. 3*C* and Fig. S3*C*). The pik1 mutants were not statistically different (P = 0.26). The extent of these delays is somewhat less than that reported for *gga1Δ gga2Δ* cells [26.1 s ± 1.9 s (5)], suggesting that Gga proteins may contribute to AP-1 recruitment through mechanisms in addition to PtdIns4P accumulation.

Another consequence of reduced PtdIns4P synthesis, observed upon inactivation of a temperature-sensitive Pik1, is a defect in TGN localization of the epsin-related adaptor Ent5, but not the homologous Ent3 (5). Accordingly, we examined whether the slower accumulation of PtdIns4P in *pik1*^{gga} and *pik1*$^{A\text{-}3A}$ cells affected Ent5-mRFP localization. In both mutants, Ent5 was more diffusely distributed and puncta were less intense than in WT (Fig. 3 *D* and *E*). In contrast, Ent3 localization was not reduced. Taken together these findings reveal that VBS1/2-mediated binding to Gga proteins plays an important role in Pik1 localization and the localized PtdIns4P accumulation that controls adaptor progression.

Functional Interaction of Mammalian PI4KIIIβ with GGA2 in Mammalian Cells. Many of the proteins involved in ccv formation at the TGN in yeast are conserved, including Pik1, Gga proteins, and AP-1. The closest mammalian homolog of Pik1 is PI4KIIIβ (12). In mammals, the GGA family is expanded to three members, GGA1–3, which serve partially overlapping functions (13–17). We tested whether GGA1–3 VHS domains interact with PI4KIIIβ in HeLa cell extracts. PI4KIIIβ preferentially bound to GGA2–VHS (Fig. 4*A*). In contrast, no specific interaction was detected between any of the GGA VHS domains and the other major PI4K at the Golgi, PI4KIIα (Fig. 4*A*). In direct binding assays, a fragment of PI4KIIIβ, which corresponds to the Gga-binding region of Pik1, displayed higher levels of binding to GGA2–VHS compared with GGA1 or GGA3 VHS (Fig. 4*B* and Fig. S4*A*). These findings indicate that PI4KIIIβ interacts preferentially with the GGA2–VHS domain, providing evidence that the ability of Gga proteins to interact with a PI4K is conserved.

To examine whether GGA proteins play a role in PI4KIIIβ localization, each of the GGA proteins was depleted by RNA interference (Fig. S4*B*). Consistent with the binding specificity of PI4KIIIβ for GGA2–VHS, only depletion of GGA2 resulted in significant mislocalization of PI4KIIIβ from the perinuclear distribution characteristic of WT cells (Fig. 4*C*). In GGA2-depleted cells, the patterns of GGA3, AP-1, and *cis*-Golgi protein GM130 were not significantly changed relative to control cells, demonstrating that the PI4KIIIβ localization defect was not the result of a global disruption of Golgi structure (Fig. 4*C* and Fig. S4*D*). Additionally, PI4KIIIβ distribution was not affected by depletion of AP-1 (Fig. 4*D* and Fig. S4*C*). The PI4KIIIβ localization defect was attributable to reduced levels of GGA2 and not off-target effects based on the observation that perinuclear localization of PI4KIIIβ was restored in GGA2-depleted cells by expression of a siRNA-resistant GGA2 gene (Fig. 4*E*). These results suggest that, in analogy to yeast Gga proteins, mammalian GGA2 plays a specific role in recruitment of PI4KIIIβ to Golgi membranes.

Discussion

Phosphoinositides serve as key determinants of membrane specificity for assembly of protein-trafficking machinery at organelles of the late secretory and endocytic pathways (18, 19). Consequently, mechanisms responsible for compartment-specific localization of phosphoinositide kinases are vital to the network of trafficking pathways that emanate from these organelles. In this study we have defined sequence motifs in Pik1 that mediate interaction with Gga proteins. This interaction directs Pik1 to the TGN for synthesis of PtdIns4P that contributes to recruitment of clathrin adaptors AP-1 and Ent5. Our data also provide evidence for specific recruitment of PI4KIIIβ by GGA2 in mammalian cells. These findings reveal an evolutionarily conserved role for GGA adaptors in regulating PtdIns4P synthesis at the TGN.

In yeast, at least two proteins participate in Pik1 localization to the TGN: Gga2 and the calcium-binding protein frequenin (Frq1) (5, 20, 21). Frq1 binds to Pik1 at sequences upstream and nearby VBS1 and VBS2 (Fig. S1*A*) (20, 22). Several observations suggest that binding to both Frq1 and Gga2 is important for Pik1 function in TGN ccv formation (5): coupled overexpression of Frq1 and Pik1 accelerated accumulation of PtdIns4P and recruitment of AP-1 and Ent5 at the TGN, Frq1 was recruited to the TGN concomitantly with Gga2p, and Gga2–VHS was able to affinity purify both Pik1 and Frq1 from lysates, likely as a

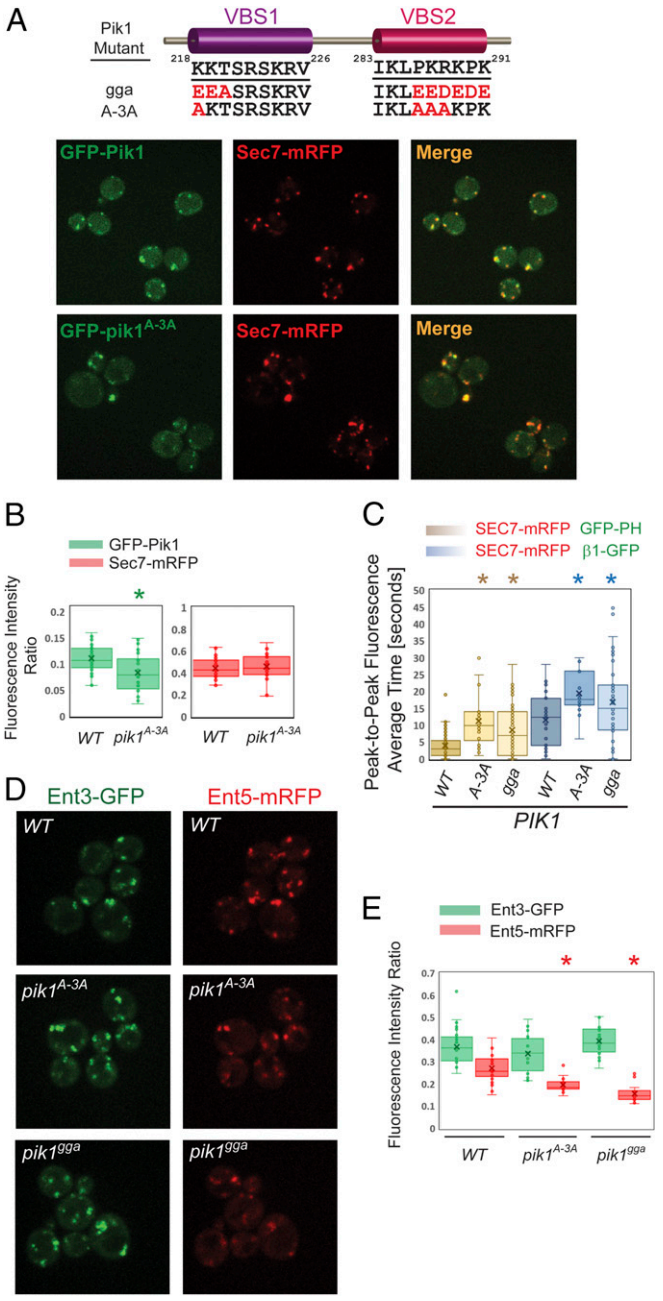

Fig. 3. Gga-binding mutations in Pik1 impair Pik1 localization, PtdIns4P accumulation, and adaptor recruitment. (*A*) Defective localization of pik1$^{A\text{-}3A}$. Diagram at top shows mutations in *pik1* alleles; *Lower* panels show representative images of strains (GPY5065, GPY5066) expressing the indicated proteins, acquired at 100× magnification by spinning disk confocal microscopy of live cells. (*B*) Localization of pik1$^{A\text{-}3A}$ is reduced. Bar and whisker plots of the indicated strains from *A* and isogenic strains, depicting fluorescence intensity ratios of GFP-Pik1 puncta to whole cells (*Left*) or Sec7-mRFP puncta to whole cells (*Right*). *$P < 0.05$ compared with WT by Student *t* test. Each point represents the average relative intensity of puncta to the whole cell in a still image of a field of cells; $n = 40$ images for WT, $n = 33$ images for *pik1*$^{A\text{-}3A}$. "x" represents mean. (*C*) Accumulation of PtdIns4P and recruitment of AP-1 are delayed in *pik1* mutant cells. Bar and whisker plots depicting times between peaks of fluorescence intensity (peak-to-peak fluorescence) of Sec7-mRFP and GFP-PH^{OSH1} (tan bars) or AP-1 β1-GFP (blue bars) in cells carrying *PIK1* (WT) or the indicated mutant *pik1* alleles. *$P < 0.05$ compared with WT by Student *t* test. Each point represents a puncta; $n = 41$ for *SEC7-mRFP GFP-PH*^{OSH1} *WT* (GPY4938), $n = 18$ for *pik1*$^{A\text{-}3A}$ (GPY5070), $n = 51$ for *pik1*^{gga} (GPY5071), $n = 27$ for *SEC7-mRFP APL2-GFP WT* (GPY4934), $n = 19$ for *pik1*$^{A\text{-}3A}$ (GPY5072), $n = 47$ for *pik1*^{gga} (GPY5073). "x" represents the mean. (*D*) Localization of Ent5-mRFP in *pik1* mutants is reduced. Representative images of Ent5-mRFP and Ent3-GFP, acquired at 100× magnification by spinning disk confocal microscopy of live WT (*PIK1*, GPY3912) or *pik1* mutant cells (GPY5074, GPY5075). (*E*) Bar and whisker plots depicting fluorescence intensity ratios of Ent3-GFP or Ent5-mRFP puncta to whole cells, displayed as in *A*. *$P < 0.00001$ compared with WT by Student *t* test. $n = 30$ images for WT (GPY3912 and isogenic strains), $n = 20$ images for *pik1*$^{A\text{-}3A}$ (GPY5074 and isogenic strains), $n = 20$ images for *pik1*^{gga} (GPY5075 and isogenic strains).

complex. Considering that Frq1 is tightly associated with Pik1 and strictly required for Pik1 TGN localization (20, 22), these results are consistent with a role for Frq1 as the primary guide for Pik1 localization to the TGN, where Gga2 binding can refine Pik1/Frq1 positioning for ccv formation. Whether there are mutual effects of Frq1 and Gga2 on Pik1 conformation and activity awaits further investigation.

Pik1 is essential for viability in yeast, with functions in clathrin-mediated traffic, late stages of secretion, and within the nucleus (5, 6, 21, 23–25). Of these processes, secretion and the nuclear function of Pik1 are necessary for cell growth (21). Importantly, in all cases except GFP-tagged forms, haploid cells expressing Pik1 Gga-binding mutants as the only version of Pik1 in the cells displayed Pik1 mutant protein levels and growth rates equivalent to WT cells, suggesting that the effects of the mutants are predominantly limited to ccv formation at the TGN.

The Gga VHS binding motifs, VBS1 and VBS2, are located in a Pik1 region predicted to be largely unstructured (26) and are characterized by multiple basic residues. This polybasic feature distinguishes VBS from the acidic nature of other known ligands of yeast Gga VHS domains, the phosphorylation-dependent sorting signal in the cargo protein Kex2 and PtdIns4P (6, 27), implying separate binding sites on VHS for Pik1 and other interacting factors. Although VBS1 and VBS2 are similar in sequence and functionally redundant, there are differences in the properties of the two motifs. In particular, there is a differential reliance on basic residues: single mutations in basic residues were sufficient to inhibit VBS1 but not VBS2 binding to Gga2–VHS. Whether this difference reflects distinct interaction sites on VHS remains to be determined.

In mammalian cells, there are two major PI4-kinases at the Golgi, PI4KIIIβ and PI4KIIα, and three partially redundant GGA proteins (14, 16, 28). We observed selective interaction of PI4KIIIβ with the VHS domain of GGA2. Furthermore, GGA2–VHS directly interacted with a region of PI4KIIIβ that corresponds to sequences in Pik1 spanning VBS1 and VBS2. The VHS-interacting region of PI4KIIIβ harbors two stretches of positive residues resembling the yeast VBS sites. However, in preliminary experiments, mutation of these residues did not disrupt binding to GGA2–VHS. Thus, the GGA–PI4K interaction is conserved between yeast and mammals but molecular details of the interaction may be distinct. This relationship is reminiscent of yeast and mammalian Gga VHS domains, which both act in cargo sorting but recognize different sorting motifs (14, 27, 29, 30).

GGA2 is necessary for PI4KIIIβ localization, defining a new function for GGA proteins in mammalian cells. The specificity of this role for GGA2 is supported by several lines of evidence in addition to the selective physical interaction: neither GGA1, GGA3, nor AP-1 depletion affected PI4KIIIβ localization, and there were no significant effects of GGA2 depletion on localization of the other Golgi/TGN proteins that were tested (GM130, GGA3, AP-1). In these ways, our results functionally distinguish GGA2 from GGA1 and GGA3, a difference that likely contributes to the distinct effects of *Gga* gene knockouts in mice, where loss of *Gga2* causes defects more severe than loss of *Gga1* or *Gga3* (16, 31).

The mechanism of PI4KIIIβ recruitment to the TGN has not been well defined. Arf1-GTP is an important contributor, but it is not clear that Arf1-GTP directly interacts with PI4KIIIβ, leading to the proposal that another factor serves as a direct

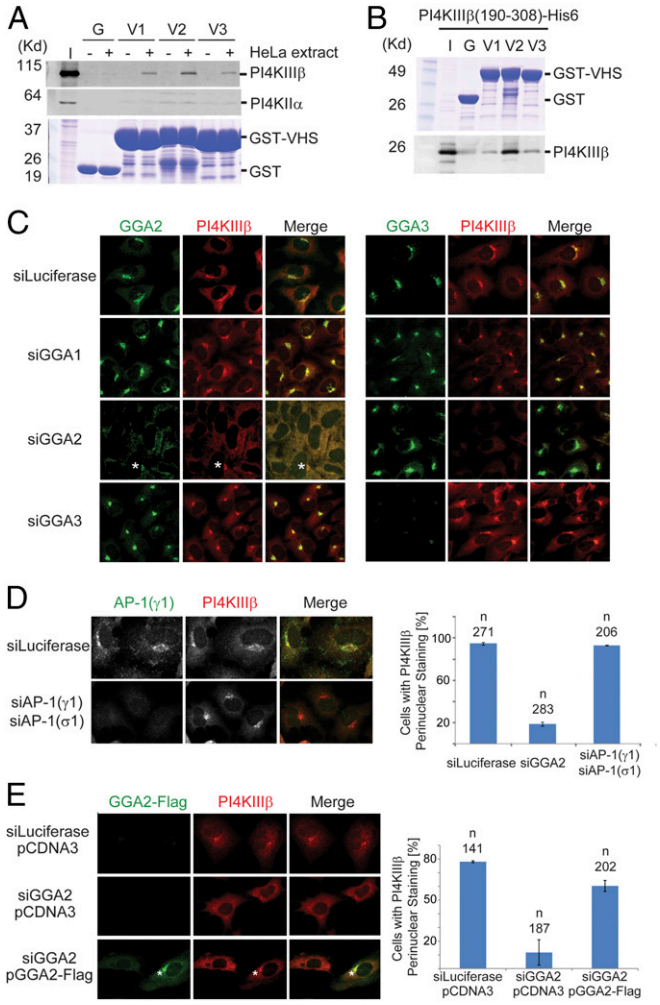

Fig. 4. Functional interaction of mammalian PI4KIIIβ and GGA2. (*A*) PI4KIIIβ interacts selectively with GGA2–VHS. HeLa cell extract (+) or buffer (–) was incubated with GST (G) or GST fused to VHS domains of GGA1 (V1), GGA2 (V2) or GGA3 (V3). Bound proteins were eluted and analyzed by SDS/PAGE and immunoblotting with anti-PI4KIIIβ (*Top*), anti-PI4KIIα (*Middle*), or staining by Coomassie blue (*Bottom*). Input (I) = 0.2%. (*B*) Purified PI4KIIIβ (190–308) was tested for binding to GST (G) or the indicated GST–VHS fusions (V1, V2, V3). Bound proteins were eluted and analyzed by SDS/PAGE and immunoblotting with anti-PI4KIIIβ. Input (I) = 3.3%. (*C*) GGA2 is required for perinuclear PI4KIIIβ localization. HeLa cells treated with siRNA targeting luciferase (siLuciferase) or the indicated GGA genes were fixed and immunostained with antibodies against PI4KIIIβ (red) and either GGA2 or GGA3 (green). An asterisk indicates a cell that retains perinuclear labeling of Gga2 and the corresponding PI4KIIIβ localization. (*D*) AP-1 is not required for PI4KIIIβ localization. (*Left*) HeLa cells treated with siLuciferase or siRNA targeting AP-1 γ1 and σ1 subunits were fixed and immunostained with antibodies against PI4KIIIβ (red) or AP-1 γ1 (green). (*Right*) Effects of siRNA targeting GGA2 or AP-1 were quantified as the percentage of cells with perinuclear PI4KIIIβ staining. *n* = number of cells. Error bars indicate SE. (*E*) PI4KIIIβ localization defect in siGGA2 cells is rescued by GGA2 expression. HeLa cells were treated with the indicated siRNA followed by transfection with vector alone (pCDNA3) or vector expressing siGGA2-resistant Flag-tagged GGA2. Cells were analyzed by immunofluorescence and PI4KIIIβ localization was quantified as in *D*. An asterisk highlights perinuclear labeling of Gga2-Flag with corresponding localization of PI4KIIIβ. All microscopy images acquired at 40× magnification.

PI4KIIIβ receptor on Golgi membranes (32). Our results suggest that the unidentified factor is GGA2. The dependence of GGA2 on Arf1-GTP for TGN localization can account for the in vitro requirement for Arf1-GTP in PI4KIIIβ recruitment and the in vivo sensitivity of PI4KIIIβ localization to brefeldin A (32), which inhibits Arf1 nucleotide exchange. Acyl-CoA binding domain containing protein 3 (ACBD3) has also been implicated in PI4KIIIβ localization (33). It may be that there are cell-type variations in PI4KIIIβ localization and multiple factors required in individual cells.

Our studies in yeast provide evidence that Gga-mediated Pik1 localization directs PtIns4P accumulation at the TGN to regulate the timing of AP-1 recruitment. Although the key proteins and interactions are conserved in mammalian cells, the relationship between GGA proteins, PI4-kinases, and AP-1 at the TGN is likely to be more complicated. In addition to PI4KIIIβ, PI4KIIα also localizes to the TGN as well as endosomes (10, 34, 35), and there are three GGA proteins with overlapping distribution and functions (13, 15–17). Furthermore, a functional interaction between AP-1 and PI4KIIα has been reported (10). Indeed, consistent with the complexity of the system, the reported effects of depleting individual PI4K on AP-1 localization have differed and sometimes conflicted (10, 36, 37). Additional investigation, including analysis of adaptor dynamics, will be needed to define the regulatory networks that couple PtdIns4P synthesis to adaptor recruitment at the mammalian TGN.

There are several examples of multimeric clathrin adaptor complexes associating with a PI kinase that produces the particular phosphoinositide selectively recognized by that adaptor complex. Specifically, physical and functional interactions have been described between AP-3 and PI4KIIα, AP-2 and PI4P5KIγ, and AP-1 and PI4KIIβ (37–39). Our data now demonstrate that this property extends to GGA2 and PI4KIIIβ. Thus, we propose that adaptor binding to phosphoinositide kinases represents a general principle in ccv formation, providing a positive feedback mechanism by which an adaptor sculpts the local phosphoinositide landscape to promote clathrin coat assembly.

Materials and Methods

Strains and Plasmids. Strains used for this study (Table S1) were derived from diploid yeast or haploid crosses using standard yeast genetic techniques and grown in standard rich (YPD) or synthetic (SD) dextrose media (described in *SI Materials and Methods*). Protein tags were introduced at the corresponding gene locus by homologous recombination (40, 41). All tagged genes were functional as described in Daboussi et al. (5). Antibodies are described in *SI Materials and Methods*. Plasmids used in this study are listed in Table S2 and described in *SI Materials and Methods*.

Protein Purification and Affinity Binding. GST fusions to yeast or mammalian GGA VHS domains and His-tagged Pik1 or PI4KIIIβ fragments were expressed in bacteria and purified using glutathione-Sepharose or NiNTA agarose as described in *SI Materials and Methods*. Purified Pik1 or PI4KIIIβ fragments were incubated in 1-mL final volume with GST-fusions immobilized on glutathione-Sepharose (*SI Materials and Methods*). To elute bound fragments, beads were suspended in 2× sample buffer [125 mM Tris·HCl pH 6.8, 4% (wt/vol) SDS, 20% (vol/vol) glycerol, 0.8% β-mercaptoethanol, 0.2 mg/mL bromophenol blue], heated to 100 °C and the samples subjected to SDS/PAGE and immunoblotting or staining with Coomassie blue.

Cell Lysates and Affinity Binding. For affinity binding with yeast lysates, exponentially growing cells were converted to spheroplasts then lysed in nondenaturing buffer (50 mM Hepes pH 7.4, 50 mM NaCl, 1% Triton X-100, 1 mM PMSF, and 1/100 Protease Inhibitor Mixture) as described in *SI Materials and Methods*. Lysate samples were incubated with GST-fusions coupled to glutathione-Sepharose for 2 h at 4 °C with rotation, and beads were washed twice with Pik1 lysis buffer and twice with Pik1 lysis buffer containing 0.1% Triton X-100. Proteins were eluted with 2× sample buffer and analyzed by SDS/PAGE and immunoblotting or staining with Coomassie blue.

For affinity binding with HeLa cell lysates, confluent cells were lysed with nondenaturing buffer (50 mM Tris·HCl pH 7.4, 150 mM NaCl, 1 mM EDTA, 1% Nonidet P-40, 0.25% sodium deoxycholate, 1 mM PMSF, and 1/100 Protease Inhibitor Mixture) as described in *SI Materials and Methods*. Lysates were brought to 0.1% SDS, then incubated with GST-fusions coupled to glutathione-Sepharose for 2 h at 4 °C with rotation. Beads were washed twice with the cell lysis buffer + 0.1% SDS, then twice with lysis buffer containing 0.1% Nonidet P-40. Proteins were eluted and analyzed as described above.

Fluorescence Microscopy. Yeast cells were grown in supplemented SD media to a density of 0.1–0.3 OD_{600} and analyzed by spinning disk microscopy, as

CELL BIOLOGY

described in Daboussi et al. (5). Images were acquired using Slidebook software v5.0, 5.5 and 6.0 (3i Intelligent Imaging Innovations). Imaging and quantification were performed with the identity of the samples blinded to the investigator.

Fluorescence intensity ratios were obtained from still images and processed using Slidebook 6.0 software as follows. For each field of cells, three masks were generated. A first mask covered the cells in full and provided the total fluorescence intensity. Two other masks were generated by manually fitting to the intracellular puncta in the GFP or RFP channels. The ratio was obtained through division of the intensity of the puncta by the total intensity of the cells in the respective channel.

For immunofluorescence analysis, HeLa cells grown on glass coverslips were fixed in 4% (wt/vol) paraformaldehyde, 4% sucrose, 0.42% 10N NaOH, 1 mM $MgCl_2$, 100 mM KH_2PO_4). Coverslips were washed in 1× PBS pH 7.4, and incubated with 0.2% Triton X-100 in PBS pH 7.4 for 10 min at room temperature. Cells were then washed in 1× PBS, treated with 10% (vol/vol) goat serum for 10 min, followed by incubation with the appropriate primary antibody at 1/100 dilution in 1× PBS for 12–16 h at 4 °C. Samples were then washed in 1× PBS and incubated with goat anti-mouse Alexa Fluor-488 or goat anti-rabbit Alexa Fluor-568 1/1,000 (Invitrogen) for 2 h at room temperature, washed with 1× PBS, and imaged by confocal microscopy.

RNA Interference. siRNA used in this study are described in Table S3. HeLa cells were plated at 25% confluence and allowed to adhere for 3 h in DMEM supplemented with 10% (vol/vol) FBS. Then siRNAs were added to a final concentration of 8 nM. Fresh media without siRNA replaced the original media 72 h after the beginning of the transfection and 24 h later cells were harvested and processed for cell lysis or immunofluorescence microscopy.

For siGGA2 rescue experiments using siRNA-resistant GGA2, HeLa cells were plated at 25% density on glass coverslips and allowed to adhere for 3 h. Then siRNA was added to a final concentration of 16 nM. After 24 h, 1 μmol of either empty vector (pcDNA-3.1) or pcDNA3-siRNA-GGA2-Flag was added to each well with 6 μL of 1 mg/mL linear polyethylenimine. Cells were incubated for 12–16 h, followed by replacement with fresh media, and addition of a second round of siLuciferase or siGGA2. Cells were washed and fixed as described below, 72 h after the first transfection.

ACKNOWLEDGMENTS. We thank Alexander van der Bliek, Matthew Denholtz, Sanjeet Patel, Kathrin Plath, John Colicelli, Laurence Meloty-Kapella, and Gerry Weinmaster for reagents and advice. This work was supported by NIH National Research Service Award T32 GM-007104 and a University of California, Los Angeles Dissertation Year Fellowship (to L.D.), and NIH Award GM39040 (to G.S.P.).

1. McMahon HT, Boucrot E (2011) Molecular mechanism and physiological functions of clathrin-mediated endocytosis. *Nat Rev Mol Cell Biol* 12(8):517–533.
2. Paczkowski JE, Richardson BC, Fromme JC (2015) Cargo adaptors: Structures illuminate mechanisms regulating vesicle biogenesis. *Trends Cell Biol* 25(7):408–416.
3. Traub LM (2005) Common principles in clathrin-mediated sorting at the Golgi and the plasma membrane. *Biochim Biophys Acta* 1744(3):415–437.
4. Robinson MS (2015) Forty years of clathrin-coated vesicles. *Traffic* 16(12):1210–1238.
5. Daboussi L, Costaguta G, Payne GS (2012) Phosphoinositide-mediated clathrin adaptor progression at the trans-Golgi network. *Nat Cell Biol* 14(3):239–248.
6. Demmel L, et al. (2008) The clathrin adaptor Gga2p is a phosphatidylinositol 4-phosphate effector at the Golgi exit. *Mol Biol Cell* 19(5):1991–2002.
7. Hirst J, Motley A, Harasaki K, Peak Chew SY, Robinson MS (2003) EpsinR: An ENTH domain-containing protein that interacts with AP-1. *Mol Biol Cell* 14(2):625–641.
8. Mills IG, et al. (2003) EpsinR: An AP1/clathrin interacting protein involved in vesicle trafficking. *J Cell Biol* 160(2):213–222.
9. Wang J, et al. (2007) PI4P promotes the recruitment of the GGA adaptor proteins to the *trans*-Golgi network and regulates their recognition of the ubiquitin sorting signal. *Mol Biol Cell* 18(7):2646–2655.
10. Wang YJ, et al. (2003) Phosphatidylinositol 4 phosphate regulates targeting of clathrin adaptor AP-1 complexes to the Golgi. *Cell* 114(3):299–310.
11. McDonold CM, Fromme JC (2014) Four GTPases differentially regulate the Sec7 Arf-GEF to direct traffic at the *trans*-Golgi network. *Dev Cell* 30(6):759–767.
12. Balla A, Balla T (2006) Phosphatidylinositol 4-kinases: Old enzymes with emerging functions. *Trends Cell Biol* 16(7):351–361.
13. Boman AL, Zhang Cj, Zhu X, Kahn RA (2000) A family of ADP-ribosylation factor effectors that can alter membrane transport through the *trans*-Golgi. *Mol Biol Cell* 11(4):1241–1255.
14. Bonifacino JS (2004) The GGA proteins: Adaptors on the move. *Nat Rev Mol Cell Biol* 5(1):23–32.
15. Dell'Angelica EC, et al. (2000) GGAs: A family of ADP ribosylation factor-binding proteins related to adaptors and associated with the Golgi complex. *J Cell Biol* 149(1): 81–94.
16. Govero J, Doray B, Bai H, Kornfeld S (2012) Analysis of Gga null mice demonstrates a non-redundant role for mammalian GGA2 during development. *PLoS One* 7(1): e30184.
17. Hirst J, et al. (2000) A family of proteins with gamma-adaptin and VHS domains that facilitate trafficking between the *trans*-Golgi network and the vacuole/lysosome. *J Cell Biol* 149(1):67–80.
18. Behnia R, Munro S (2005) Organelle identity and the signposts for membrane traffic. *Nature* 438(7068):597–604.
19. Di Paolo G, De Camilli P (2006) Phosphoinositides in cell regulation and membrane dynamics. *Nature* 443(7112):651–657.
20. Hendricks KB, Wang BQ, Schnieders EA, Thorner J (1999) Yeast homologue of neuronal frequenin is a regulator of phosphatidylinositol-4-OH kinase. *Nat Cell Biol* 1(4): 234–241.
21. Strahl T, Hama H, DeWald DB, Thorner J (2005) Yeast phosphatidylinositol 4-kinase, Pik1, has essential roles at the Golgi and in the nucleus. *J Cell Biol* 171(6):967–979.
22. Strahl T, et al. (2007) Structural insights into activation of phosphatidylinositol 4-kinase (Pik1) by yeast frequenin (Frq1). *J Biol Chem* 282(42):30949–30959.
23. Flanagan CA, et al. (1993) Phosphatidylinositol 4-kinase: Gene structure and requirement for yeast cell viability. *Science* 262(5138):1444–1448.
24. Hama H, Schnieders EA, Thorner J, Takemoto JY, DeWald DB (1999) Direct involvement of phosphatidylinositol 4-phosphate in secretion in the yeast *Saccharomyces cerevisiae*. *J Biol Chem* 274(48):34294–34300.
25. Walch-Solimena C, Novick P (1999) The yeast phosphatidylinositol-4-OH kinase pik1 regulates secretion at the Golgi. *Nat Cell Biol* 1(8):523–525.
26. Burke JE, et al. (2014) Structures of PI4KIIIβ complexes show simultaneous recruitment of Rab11 and its effectors. *Science* 344(6187):1035–1038.
27. De M, Abazeed ME, Fuller RS (2013) Direct binding of the Kex2p cytosolic tail to the VHS domain of yeast Gga2p facilitates TGN to prevacuolar compartment transport and is regulated by phosphorylation. *Mol Biol Cell* 24(4):495–509.
28. Balla T (2013) Phosphoinositides: Tiny lipids with giant impact on cell regulation. *Physiol Rev* 93(3):1019–1137.
29. Misra S, Puertollano R, Kato Y, Bonifacino JS, Hurley JH (2002) Structural basis for acidic-cluster-dileucine sorting-signal recognition by VHS domains. *Nature* 415(6874): 933–937.
30. Shiba T, et al. (2002) Structural basis for recognition of acidic-cluster dileucine sequence by GGA1. *Nature* 415(6874):937–941.
31. Doray B, Govero J, Kornfeld S (2014) Impact of genetic background on neonatal lethality of Gga2 gene-trap mice. *G3 (Bethesda)* 4(5):885–890.
32. Godi A, et al. (1999) ARF mediates recruitment of PtdIns-4-OH kinase-beta and stimulates synthesis of PtdIns(4,5)P2 on the Golgi complex. *Nat Cell Biol* 1(5):280–287.
33. Sasaki J, Ishikawa K, Arita M, Taniguchi K (2012) ACBD3-mediated recruitment of PI4KB to picornavirus RNA replication sites. *EMBO J* 31(3):754–766.
34. Balla A, Tuymetova G, Barshishat M, Geiszt M, Balla T (2002) Characterization of type II phosphatidylinositol 4-kinase isoforms reveals association of the enzymes with endosomal vesicular compartments. *J Biol Chem* 277(22):20041–20050.
35. Minogue S, et al. (2006) Phosphatidylinositol 4-kinase is required for endosomal trafficking and degradation of the EGF receptor. *J Cell Sci* 119(Pt 3):571–581.
36. Henmi Y, et al. (2016) PtdIns4KIIα generates endosomal PtdIns(4)P and is required for receptor sorting at early endosomes. *Mol Biol Cell* 27(6):990–1001.
37. Wieffer M, et al. (2013) PI4K2β/AP-1-based TGN-endosomal sorting regulates Wnt signaling. *Curr Biol* 23(21):2185–2190.
38. Craige B, Salazar G, Faundez V (2008) Phosphatidylinositol-4-kinase type II alpha contains an AP-3-sorting motif and a kinase domain that are both required for endosome traffic. *Mol Biol Cell* 19(4):1415–1426.
39. Krauss M, Kukhtina V, Pechstein A, Haucke V (2006) Stimulation of phosphatidylinositol kinase type I-mediated phosphatidylinositol (4,5)-bisphosphate synthesis by AP-2mu-cargo complexes. *Proc Natl Acad Sci USA* 103(32):11934–11939.
40. Janke C, et al. (2004) A versatile toolbox for PCR-based tagging of yeast genes: new fluorescent proteins, more markers and promoter substitution cassettes. *Yeast* 21(11): 947–962.
41. Longtine MS, et al. (1998) Additional modules for versatile and economical PCR-based gene deletion and modification in *Saccharomyces cerevisiae*. *Yeast* 14(10):953–961.
42. Robinson JS, Klionsky DJ, Banta LM, Emr SD (1988) Protein sorting in Saccharomyces cerevisiae: Isolation of mutants defective in the delivery and processing of multiple vacuolar hydrolases. *Mol Cell Biol* 8(11):4936–4948.
43. Yeung BG, Phan HL, Payne GS (1999) Adaptor complex-independent clathrin function in yeast. *Mol Biol Cell* 10(11):3643–3659.
44. Costaguta G, Duncan MC, Fernández GE, Huang GH, Payne GS (2006) Distinct roles for TGN/endosome epsin-like adaptors Ent3p and Ent5p. *Mol Biol Cell* 17(9):3907–3920.
45. Hirst J, et al. (2009) Spatial and functional relationship of GGAs and AP-1 in *Drosophila* and HeLa cells. *Traffic* 10(11):1696–1710.
46. Mardones GA, et al. (2007) The *trans*-Golgi network accessory protein p56 promotes long-range movement of GGA/clathrin-containing transport carriers and lysosomal enzyme sorting. *Mol Biol Cell* 18(9):3486–3501.